6.0 NONMAGNETIC SAMPLE CHARACTERIZATION

6.1 SEM imaging

Samples that did not have obvious deficiencies in their production or in their IRM acquisition curves were examined with the JEOL JSM-35CF Scanning Electron Microscope (SEM) in the Materials Engineering Department. At this stage, the goal was to micrograph the samples so that the grain size distribution could be measured and used to select samples for the TRM and PTRM measurements. A secondary goal was to correlate the observed grain size distributions with the temperature programs used during sample production. Third, the SEM provided a means to verify sample homogeneity. Sample micrographs are given in Appendix G.

Magnetite grains exceeding 1 μm could usually be identified by their distinctive octahedral [111] habit. This was usually apparent when observed in the secondary electron imaging mode and/or electron back-scatter mode. The secondary electron imaging mode was most sensitive to surface topography, and usually produced the highest-resolution micrographs. The electron back-scatter mode (in "compo" mode) is sensitive to topography as well, but is also sensitive to average atomic number. Iron has the largest atomic number in the prepared samples, so iron compounds are easily identified as the bright crystals in the electron back-scatter micrographs. Magnetite and Ca/K/Na-Fe silicates are the dominant iron-containing compounds formed (see Section 6.3). Of these, only magnetite is isometric, so only magnetite can have an octahedral habit. The greater ease in identifying magnetite in the electron back-scatter micrographs is offset by the lower resolution obtained in this mode. Both secondary electron

imaging mode and electron back-scatter mode micrographs were used, with the choice made based on whichever gave the clearest micrographs.

It was difficult to obtain focused images of magnetite grains that were much smaller than 1 μm, yet it appeared possible to focus on other crystals of similar size. Part of the problem was the selection of the low stage position for the preliminary characterizations. The low position is preferable for EDAX analysis, but less suitable for imaging. In addition, it is possible that the magnetic moment of the magnetite grains locally distorts the trajectory of the incident electron beam by a small amount, thus destroying the ability to observe fine details.

In each sample, several crystals were visually identified as magnetite, then the electron microprobe was used to confirm that they were iron oxides. The electron microprobe analyses are discussed in Section 6.2. Any octahedral iron oxide was assumed to be magnetite. Once several crystals were confirmed, it was assumed that all visually similar crystals in the micrograph were also magnetite.

Several of the samples were eliminated from further consideration at this stage. These included samples that had obvious wide variations in magnetite grain size, and samples with aberrant magnetite crystal morphology. Magnetite grain sizes were measured for selected micrographs from each remaining sample. The magnification was chosen to facilitate measuring the magnetite grains, and would typically result in about 50 to 60 measurable grains per micrograph. Where possible, images of 50 grains were systematically measured with a dial caliper. Grain size was measured in two perpendicular directions, and an effective diameter defined as the geometric mean of the two measurements. Errors were introduced by image blurring, differences in effective magnification due to sample topography, partially hidden or buried grains, variations in grain orientation, and the arbitrary choice of which directions to measure the non-spherical grains. Of these, the last two are expected to have contributed the most to the error, except for sub-micron grains where image blurring dominates.

For perfect octahedra, the ratio between the diameters defined by opposite faces, opposite edges, and opposite vertices is 0.82:1.0:1.4. I measured the projected distance between two opposite edges wherever possible. Depending on the grain orientation, the measured value may be up to 18% too small, with the worst case being when grain faces were vertical. An argument can be made, based on projections of a perfect octahedron onto a plane, for using the largest of the two measurements as the effective diameter of the grain. In this case, the ratio between the expected measured grain diameter (defined by opposite edges) and the actual diameter for a randomly-oriented octahedron is given by (see Appendix E)

$$\frac{\langle d_{meas} \rangle}{d_{actual}} = \int_0^{\frac{\pi}{4}} d\theta \int_0^{\cot^{-1}\cos\theta} \sin\phi \, d\phi \int_0^{2\pi} d\varphi \left\{ 2\left(\cos^2\phi\cos^2\theta + \sin^2\theta\right)^{\frac{1}{2}} \times \right.$$

$$\left. \sin\left[\tan^{-1}\left(\frac{\sin\theta}{\cos\phi\cos\theta} \right) + \tan^{-1}\left(\frac{\cos\theta - \sin\theta}{\cos\phi(\cos\theta + \sin\theta)} \right) \right] \right\} \Big/ \int_0^{\frac{\pi}{4}} d\theta \int_0^{\cot^{-1}\cos\theta} \sin\phi \, d\phi \int_0^{2\pi} d\varphi \, \sqrt{2}$$

$$\approx 0.9675. \qquad (6.1\text{-}1)$$

This argument does not hold for non-octahedral grains, and in particular does not hold for observed grains that take the form swept out by a [111] octahedron translated slightly along one of the crystallographic axes. An alternate method is to use the geometric mean of two perpendicular "diameters". The effective grain diameters in Appendix B were calculated both ways. In any case, for an octahedral grain, the grain volume is given by

$$v = d^3\sqrt{2} \qquad (6.1\text{-}2)$$

The sample grain-size distributions were the primary means of selecting samples for the TRM and PTRM acquisition experiments. Since these experiments could potentially result in chemical alteration of the samples, the SEM observations were repeated after completing the TRM and PTRM experiments. This effectively destroyed the sample.

Table 1 summarizes the mean grain size for each of the six selected samples. To obtain a reasonable statistical sampling, one hundred grains were measured for each of the samples after the TRM experiments. Sample 023 was an exception, where only 77 measurable grains were observed in the SEM. The number of grains measured before the experiments varied, but was usually either 50 or 100. Figures 22 through 33 show the grain size distributions measured after the magnetic experiments were completed. Initial grain size distributions are given in Appendix A.1.

There is reasonable agreement between the "before" and "after" diameters measured for sample 004. The "before" measurement is based on only 19 grains in a poorly-focused photomicrograph. Sample 004 partially oxidized early in the TRM experiments. The images obtained afterward showed rounded rather than octahedral grains, so only one diameter was obtained for each grain.

Sample 006 showed excellent agreement between the "before" and "after" measurements. Well-formed octahedra were observed in both cases.

Sample 023 showed a slight decrease in measured grain diameter between the "before" and "after" measurements. The decrease is not significant at the α=0.005 level. Well-formed octahedra were observed in both the "before" and "after" photomicrographs.

Sample 001 showed a decrease in measured grain diameter between the "before" and "after" measurements. The decrease was significant at the α=0.10 level. Sample 001 was badly oxidized near the end of the TRM experiments. The images obtained afterward showed rounded rather than octahedral grains, so only one diameter was obtained for each grain. Considering the images obtained,

I suggest that the diameters obtained after the experiments might still be used, with caution, as indicators of the grain size throughout the experiments.

Sample 012 showed a significant increase in grain size between the "before" and "after" measurements. The cause of the increase is not known The "after" photomicrographs show a large number of well-defined octahedral grains, but the grains appear to have a mottled coating. The coating does not appear to be thick enough to account for more than about 10 percent of the measured diameter. Perhaps crystal growth continued during the initial thermal cycling and possibly during the thermomagnetic experiments as well. Alternately, the portions of the sample characterized before and after the TRM experiments might have come from dissimilar regions of the sample. One mechanism by which this could occur is if the two fragments corresponded to different phases in a two immiscible liquid melt, and therefore grew different size magnetite crystals.

Sample 018 showed a complete change in grains size distribution between the "before" and "after" photomicrographs. In the "before" images, there were a number of well-formed octahedra in the 5 μm range. Only a few grains of this size were observed in the "after" images. On the other hand, a large number of 1.4 μm grains were found in the "after" images. These were not seen in the "before" images, although a number of much smaller iron-rich grains were noted. These were initially thought to be Ca-Fe silicates, but may instead have been magnetite. Perhaps the portions of the sample characterized before and after the TRM experiments corresponded to different phases in a two immiscible liquid melt, and therefore grew different size magnetite crystals. An alternate explanation is that the small magnetite crystals could have grown during the precautionary thermal cycling step. (The self-consistency of the magnetic measurements discussed later argues against significant sample changes after the magnetic experiments began). In any case, the grain size variation in sample 018 is much larger than the other samples, and this can explain some of the anomalous results obtained in the TRM experiments.

Table 1 Mean grain sizes before and after experiments

Sample ID	Before TRM Experiments		After TRM Experiments	
	Geometric mean diameter	Maximum measured diameter	Geometric mean diameter	Maximum measured diameter
004	0.89 μm	1.0 μm	(0.80 μm)	0.80 μm
006	1.18 μm	1.36 μm	1.18 μm	1.25 μm
023	1.58 μm	1.66 μm	1.49 μm	1.59 μm
001	1.83 μm	2.04 μm	(1.49 μm)	1.49 μm
012	1.59 μm	1.80 μm	3.55 μm	3.61 μm
018	4.94 μm	5.75 μm	1.39 μm	1.49 μm

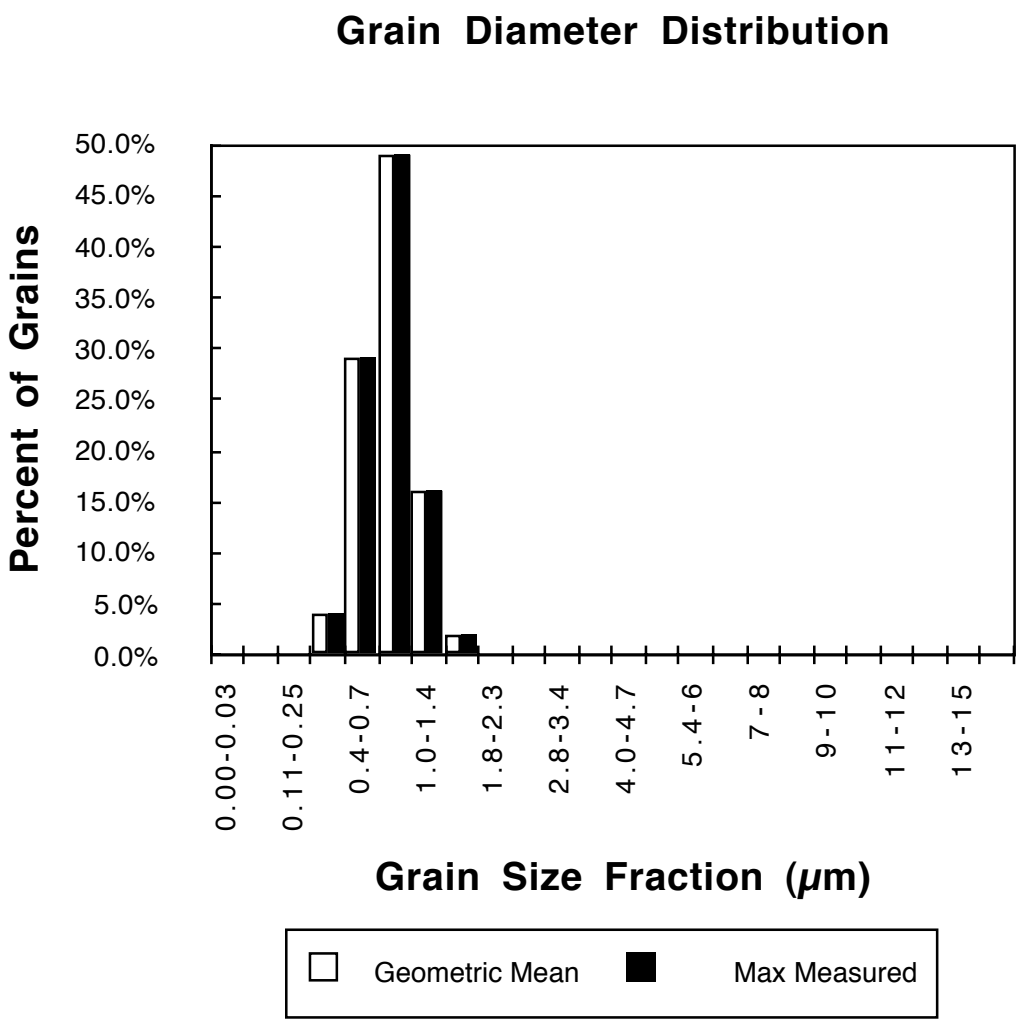

Figure 22 Sample 004 grain diameter distribution after all magnetic experiments were completed. Only one diameter was measured for each grain. The mean value was 0.80 μm for this diameter. The sample was oxidized by this time, so measurement precision was degraded.

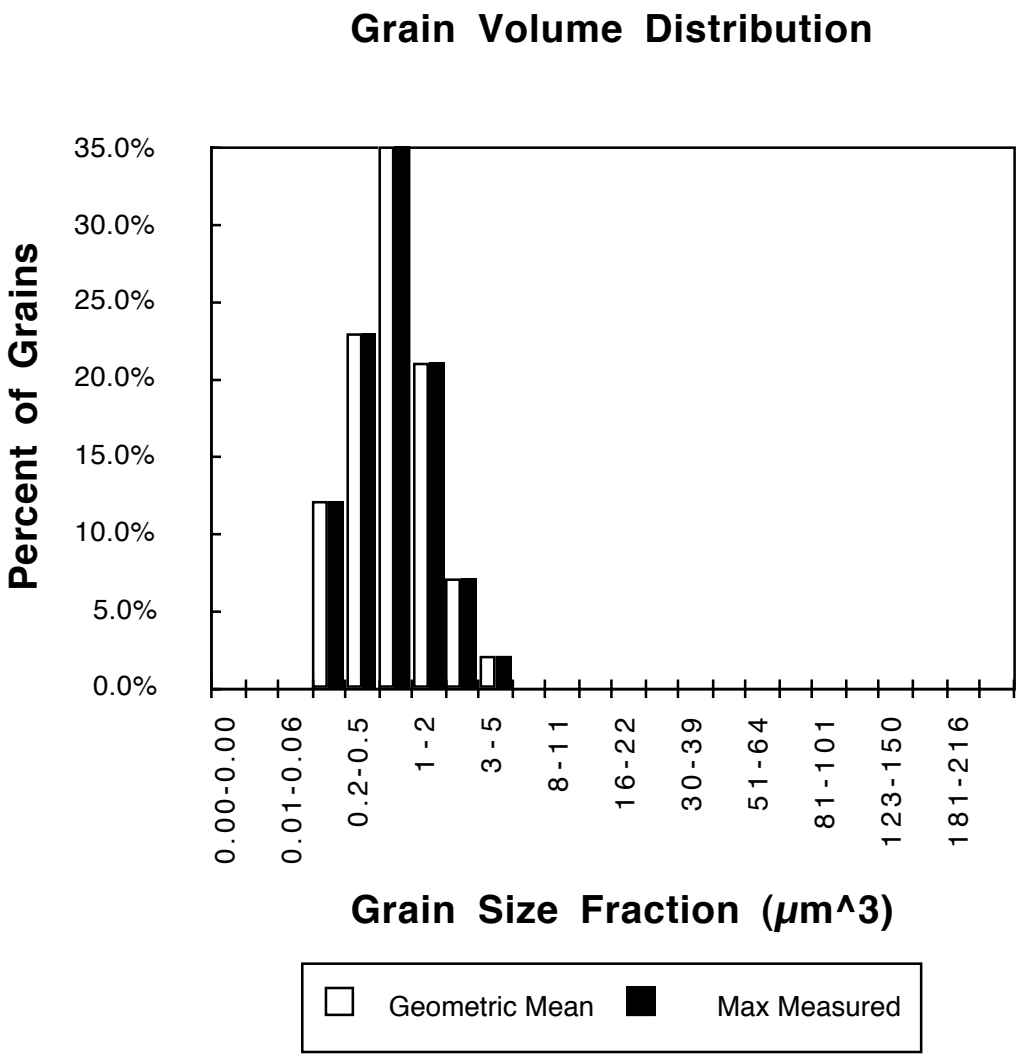

Figure 23 Sample 004 grain volume distribution after all magnetic experiments were completed. The sample was oxidized by this time, so measurement precision was degraded.

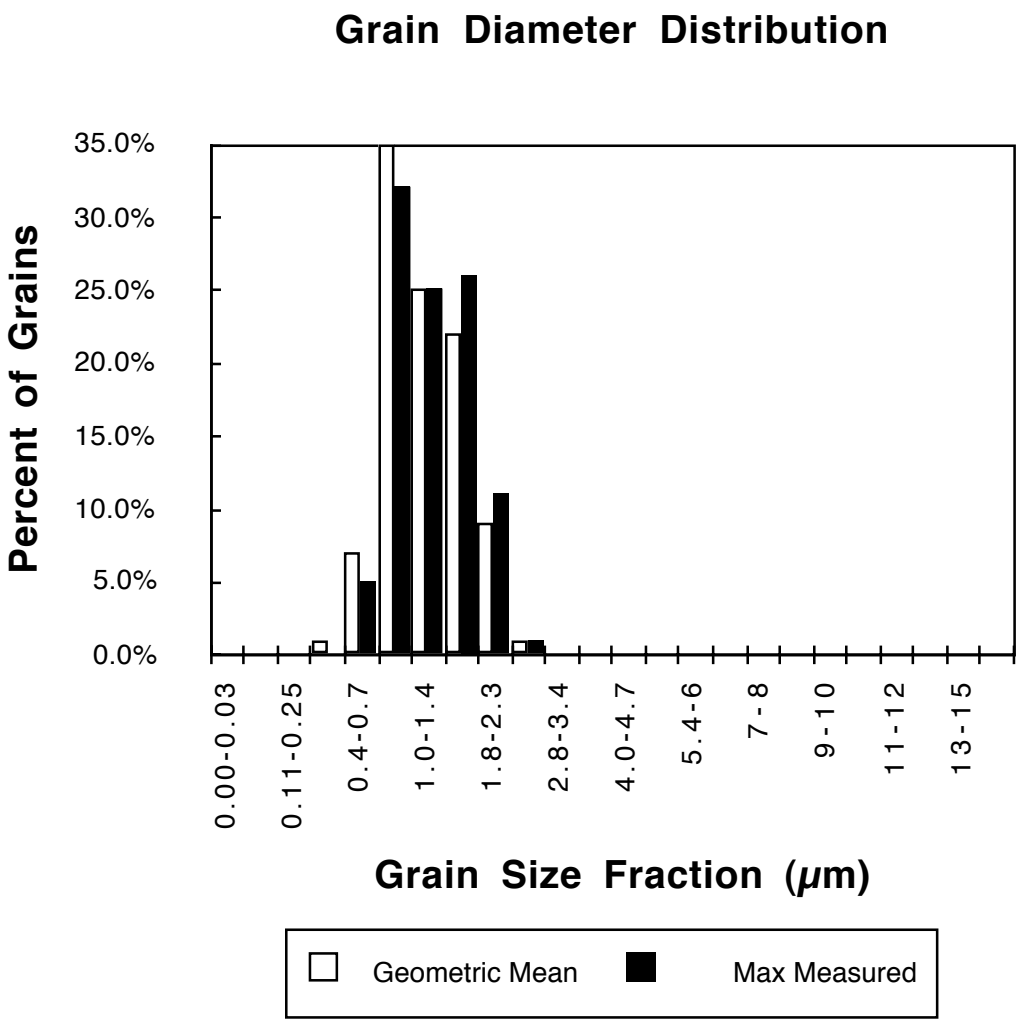

Figure 24 Sample 006 grain diameter distribution after all magnetic experiments were completed. The mean values were 1.18 and 1.25 μm for the geometric mean diameter and maximum measured diameter, respectively.

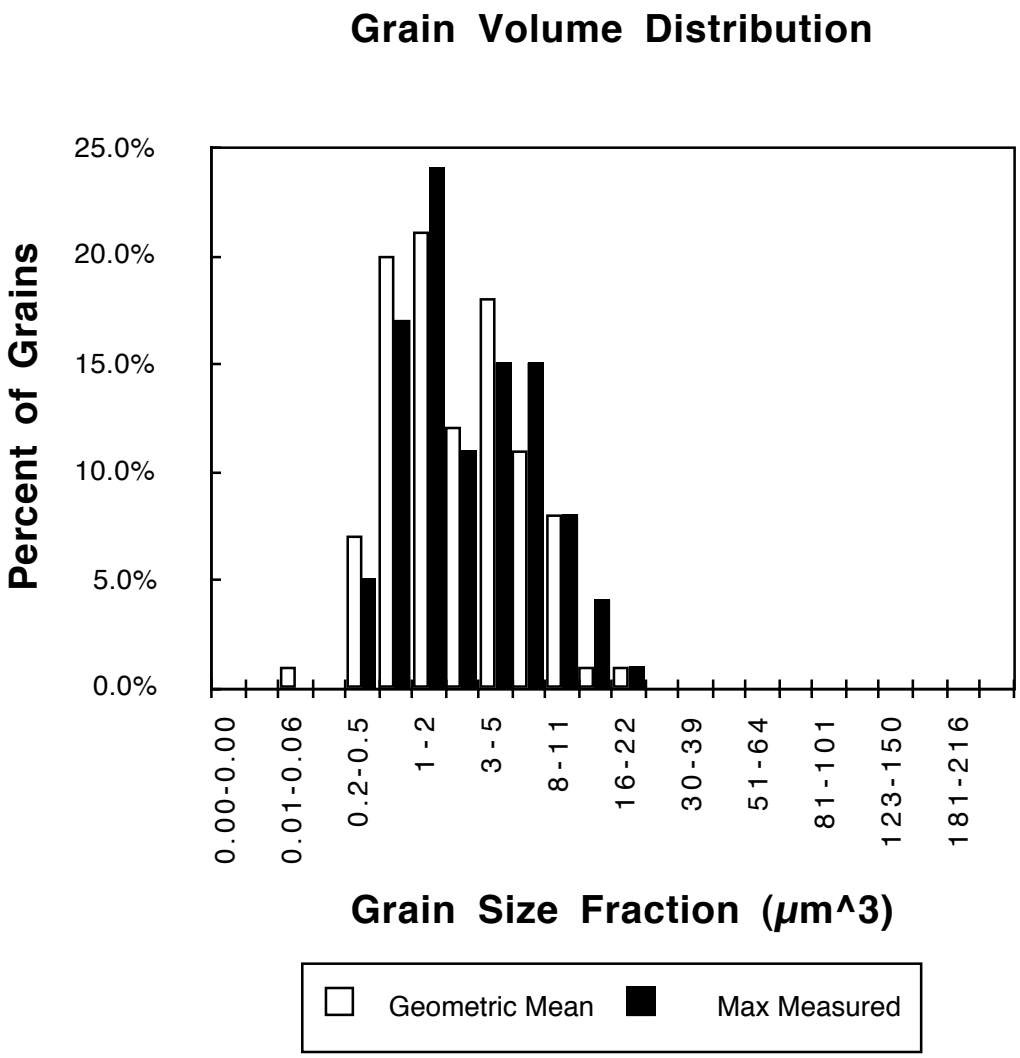

Figure 25 Sample 006 grain volume distribution after all magnetic experiments were completed.

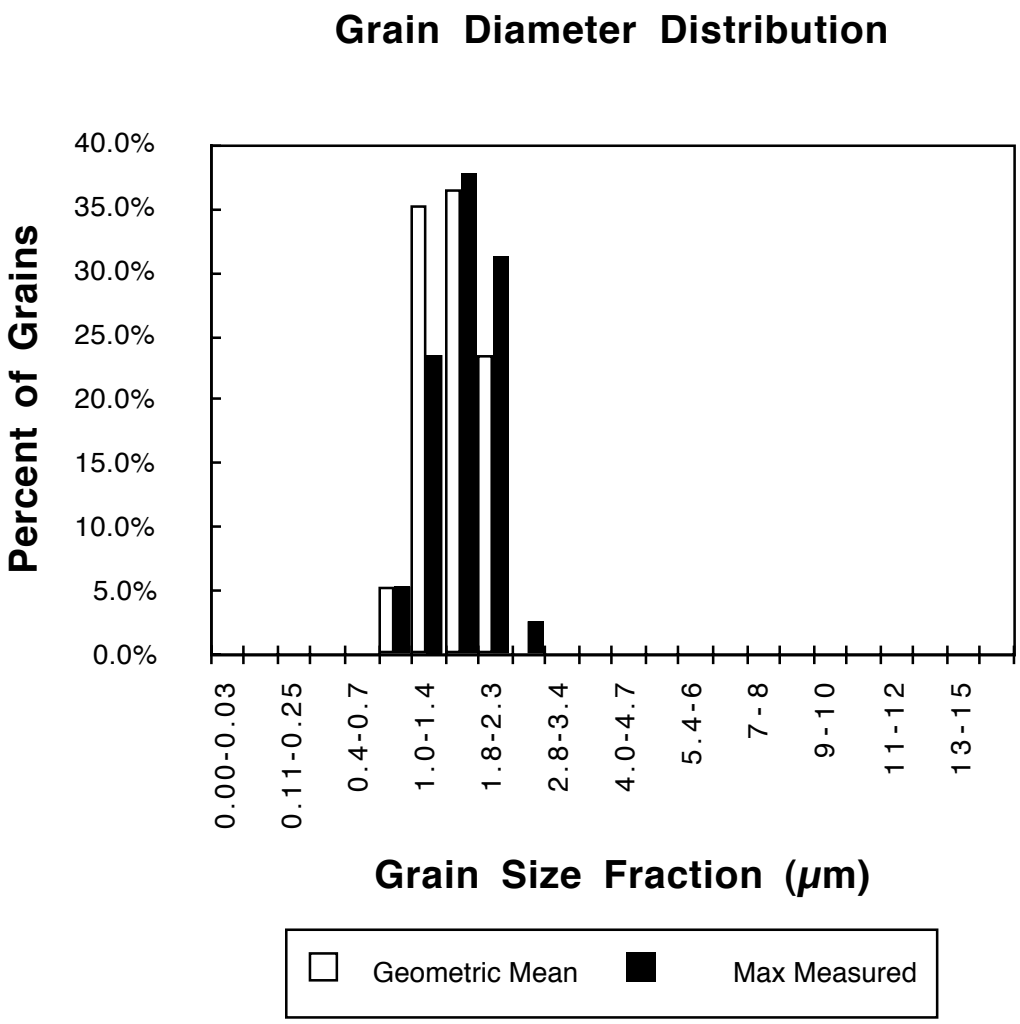

Figure 26 Sample 023 grain diameter distribution after all magnetic experiments were completed. The mean values were 1.49 and 1.59 μm for the geometric mean diameter and maximum measured diameter, respectively.

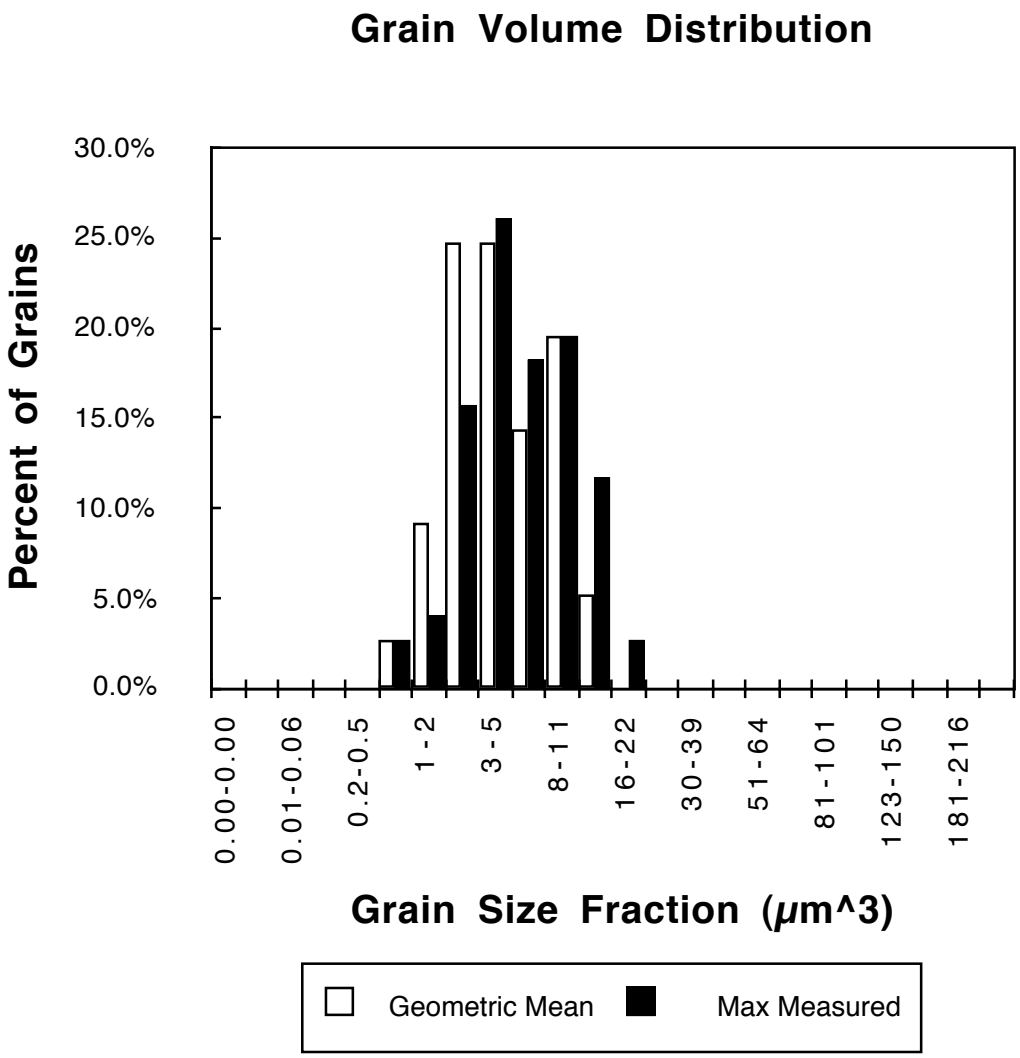

Figure 27 Sample 023 grain volume distribution after all magnetic experiments were completed.

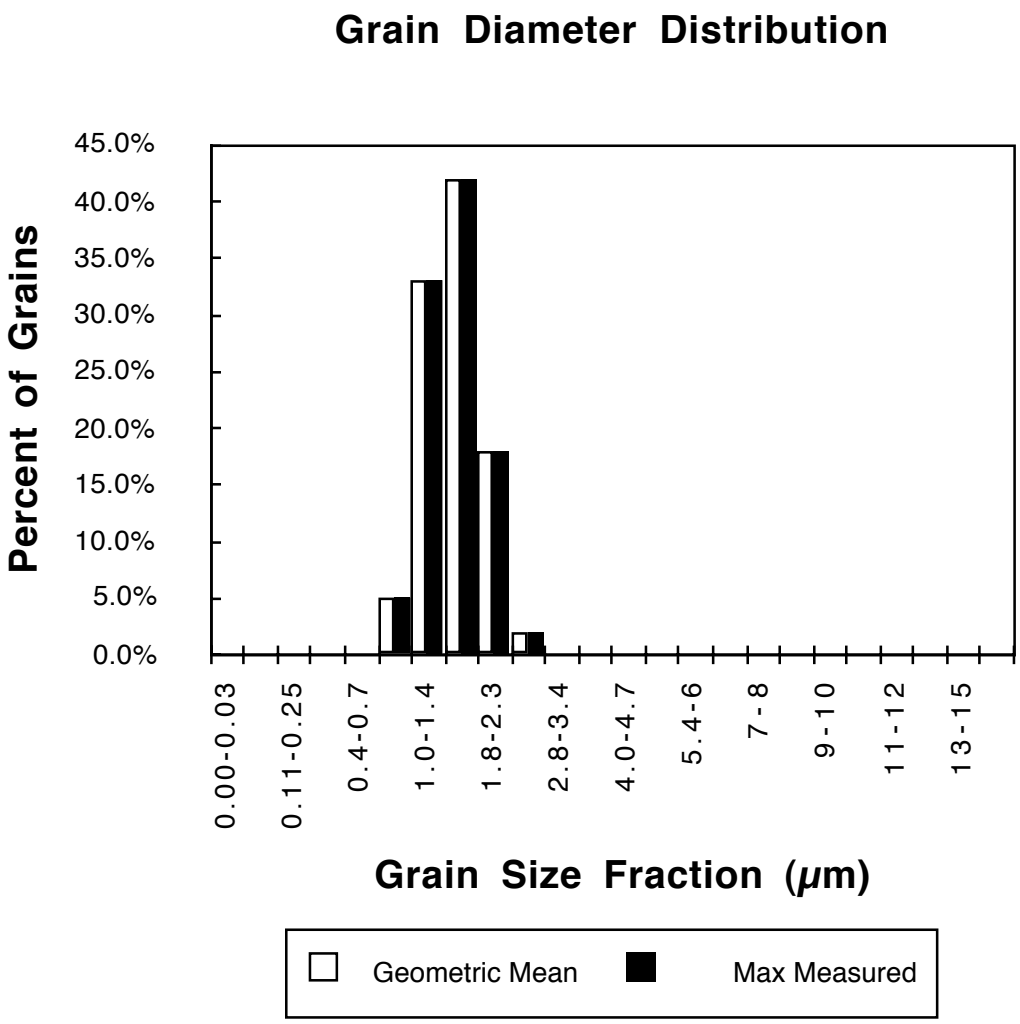

Figure 28 Sample 001 grain diameter distribution after all magnetic experiments were completed. Only one diameter was measured for each grain. The mean value was 1.49 μm for this diameter. The sample was oxidized by this time, so measurement precision was degraded.

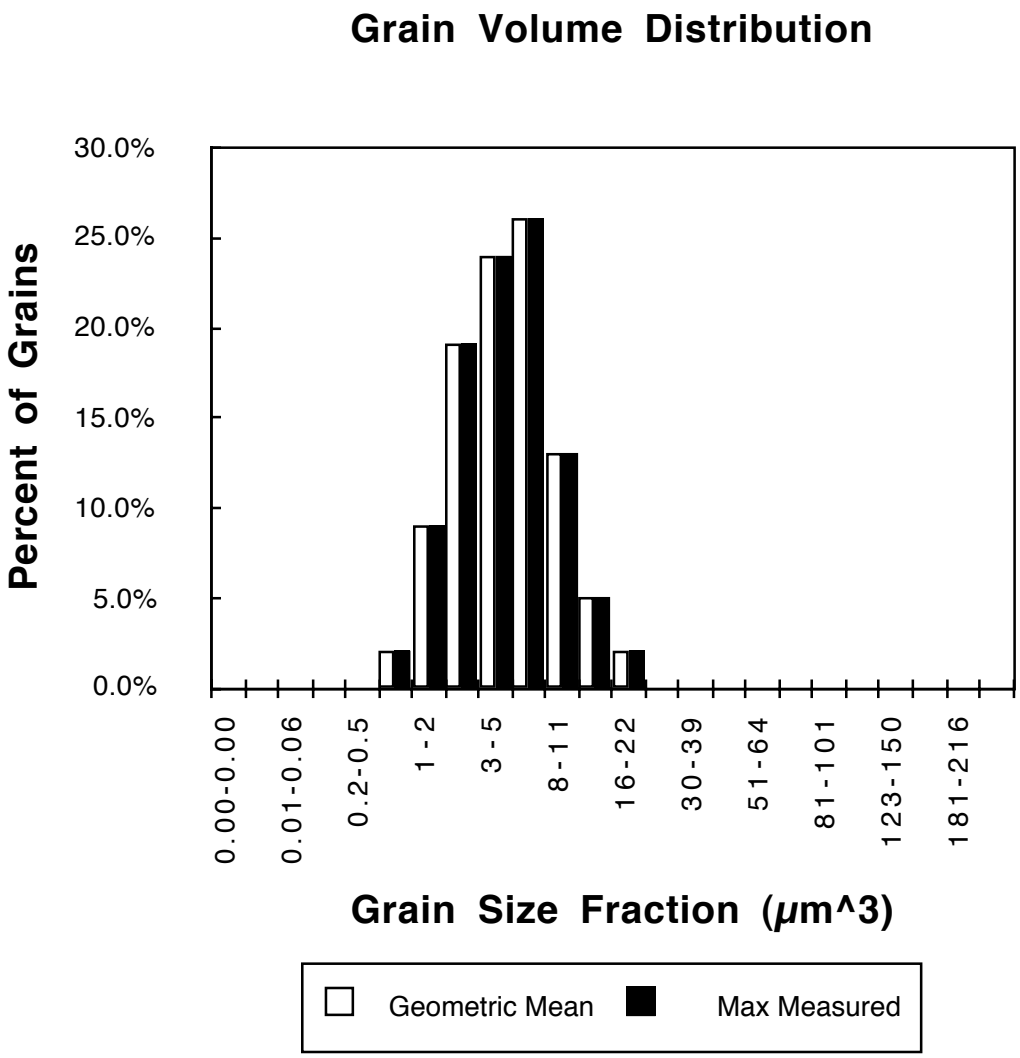

Figure 29 Sample 001 grain volume distribution after all magnetic experiments were completed. The sample was oxidized by this time, so measurement precision was degraded.

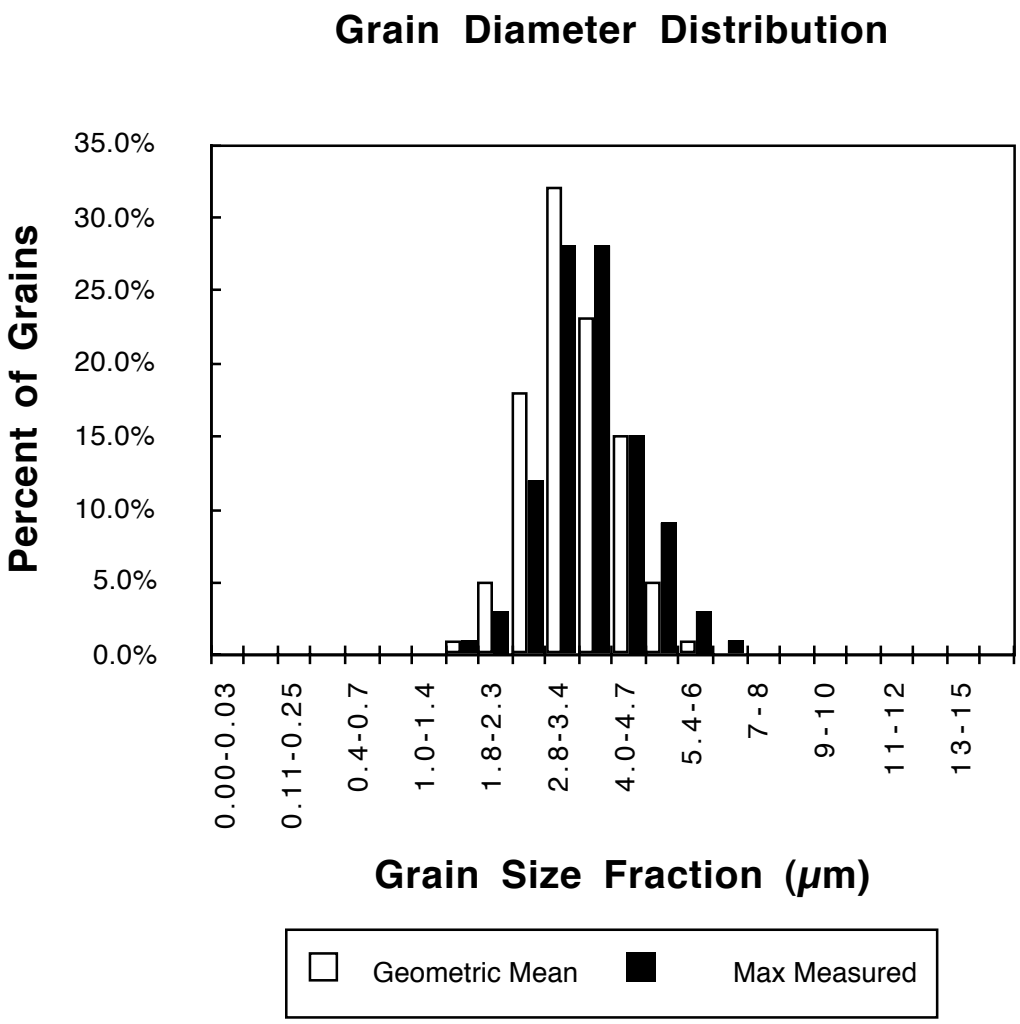

Figure 30 Sample 012 grain diameter distribution after all magnetic experiments were completed. The mean values were 3.35 and 3.62 μm for the geometric mean diameter and maximum measured diameter, respectively.

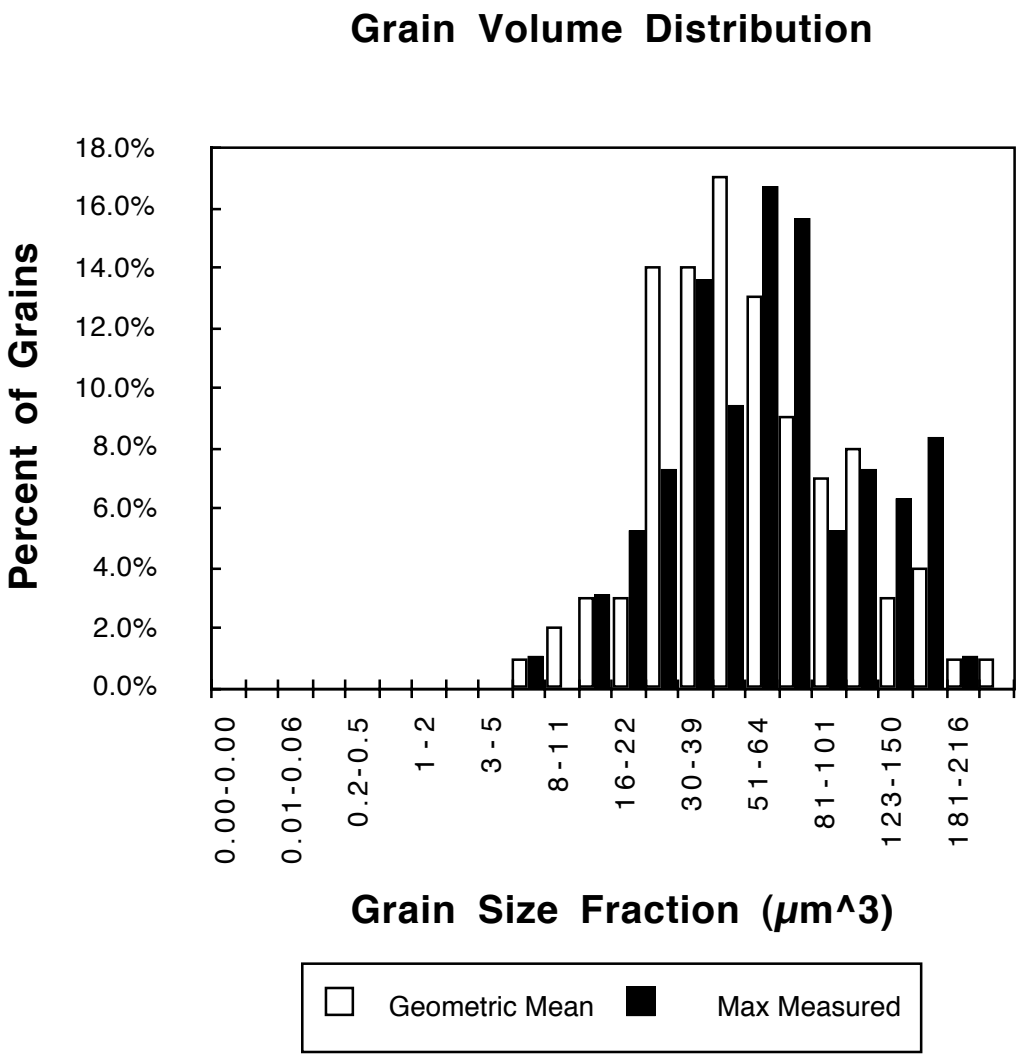

Figure 31 Sample 012 grain volume distribution after all magnetic experiments were completed.

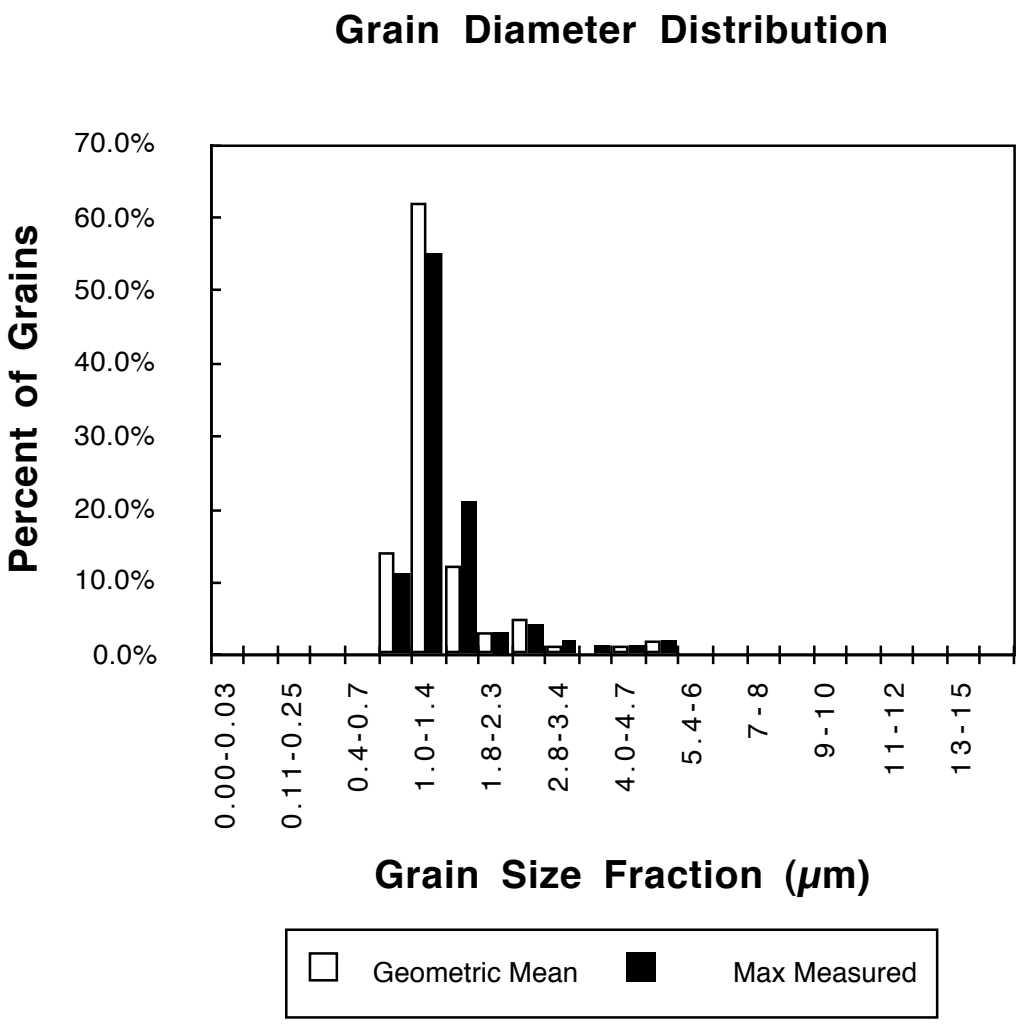

Figure 32 Sample 018 grain diameter distribution after all magnetic experiments were completed. The mean values were 1.39 and 1.49 μm for the geometric mean diameter and maximum measured diameter, respectively. Several large (≈ 5 μm) grains were noted.

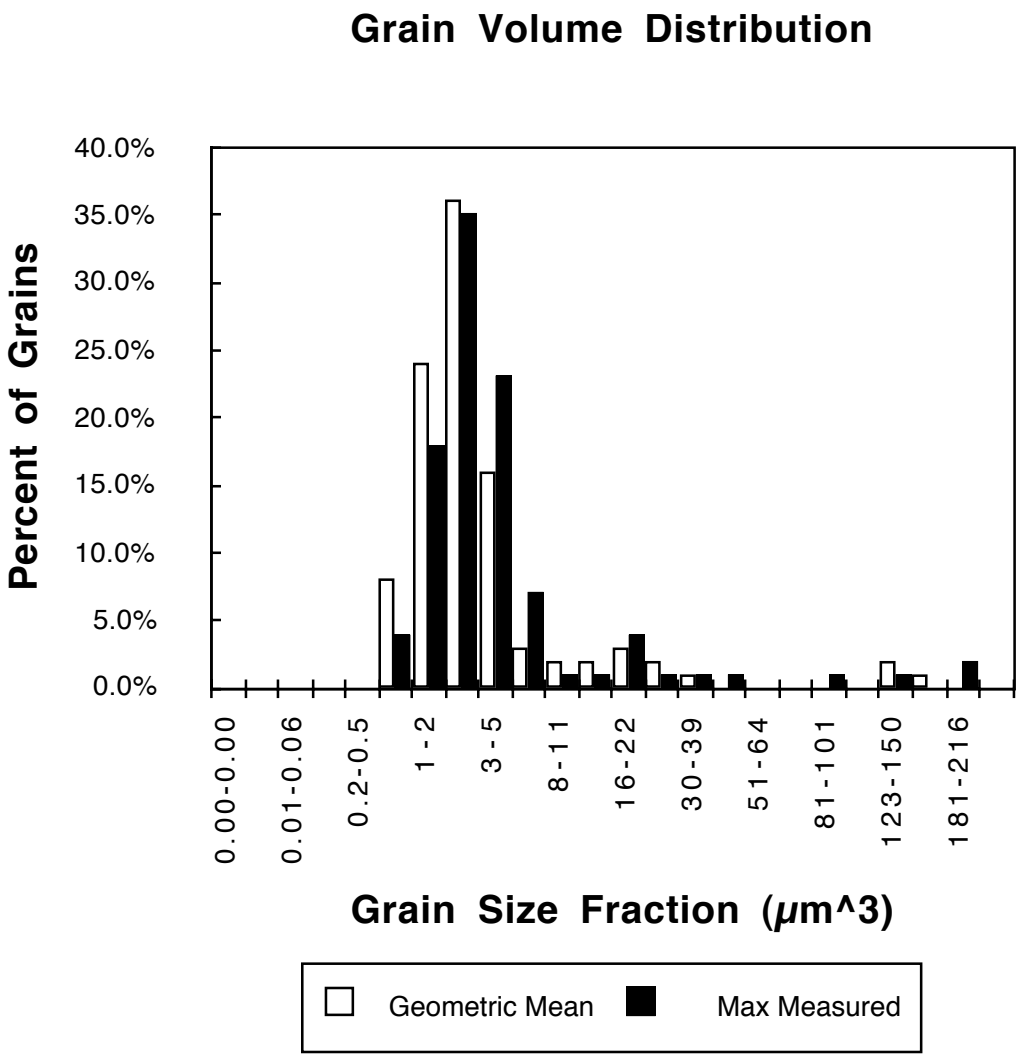

Figure 33 Sample 018 grain volume distribution after all magnetic experiments were completed.

6.2 Electron microprobe

The electron microprobe capabilities of the SEM were used to confirm the identification of suspected magnetite grains. Because the samples had a known chemical composition, no attempt was made to use the microprobe to perform quantitative chemical analyses. Furthermore, the size of the magnetite crystals was on the same order as the region activated by the electron beam, so it would have been impossible to exclude the surrounding matrix from any analyses of the magnetite crystals.

One potentially interesting observation emerged from the microprobe use: magnetite grains were often found in areas that had a higher potassium peak than the magnetite-poor regions. This supports the hypothesis that two immiscible liquids might be present in the melts used to form the samples. Pursuit of this hypothesis is outside the scope of this study.

6.3 X-Ray diffraction

Powder x-ray diffraction patterns were obtained for several of the samples with a Philips x-ray diffractometer (XRD). This proved to be more useful for identifying the phases present in the matrix than for characterizing the magnetite grains. X-ray diffraction confirmed that the samples contained magnetite, but this was known from the magnetic measurements. There was a tendency for the magnetite grains to oxidize during grinding, so the resulting patterns sometimes showed the presence of hematite or maghemite. Oxidation could have been prevented by grinding under acetone, but this was not pursued.

In this study, there was no titanium in the samples, so determining the Ulvöspinel content of the (titano-)magnetite crystals was not an issue. Since the XRD did not provide any additional quantitative information in this study, its use was discontinued. In future studies involving titanomagnetites, the XRD can be used to determine the lattice parameter of the titano-magnetites, thereby providing a measure of the Ulvöspinel content.

A final, and convincing argument for not performing x-ray diffraction on the samples used in the magnetic studies is that the samples did not contain enough material for proper XRD analysis. Furthermore, grinding the sample material to attempt to obtain an x-ray diffraction pattern would have rendered the sample unusable for SEM observation. Since the SEM observations were essential for accurate grain-size measurement and for grain shape assessments, XRD analysis was not feasible.

6.4 Optical microscopy

Optical examination was considered, but ultimately rejected because the SEM images showed that the grain sizes were near the lower limit of optical resolution, and adequate grain-size information could be obtained from the SEM images.